Supplemental data to

Time-Delayed *in vivo* Assembly of Subunit *a* into Preformed *Escherichia coli* F_OF_1-ATP Synthase

Britta Brockmann, Kim Danielle Koop genannt Hoppmann, Henrik Strahl, Gabriele Deckers-Hebestreit

Abteilung Mikrobiologie, Fachbereich Biologie/Chemie, Universität Osnabrück, D-49069 Osnabrück, Germany

TABLE S1 Primers for real-time RT-PCR and mutagenesis

Primer number	Primer name	Sequenz (5' → 3')	Annealing in pBWU13
1	RT3-s	CAG GCG CAG GCG GAA ATT G	1626-1645
2	atpF-rev	CCG TAA TAA ATT CAG ACA TCA GCC CC	1821-1796
3	atpA1-for	GCG AAC TGA TCA AGC AGC GC	2374-2393
4	RT6-as	ACC CAT AAC AAC CGC ACC TAC	2579-2559
5	rpsL-for	GGT ACG CAA ACC ACG TGC TCG	--
6	rpsL-rev	CAG GTT GTG ACC TTC ACC ACC	--
7	atpI-KpnI-for	CGT GGG TTT TGG T**A**C **C**GG TGG TTC AG	85-110
8	atpI-KpnI-rev	CTG AAC CAG C**G**G **T**AC CAA AAC CCA CG	110-85
9	D_atpB_s	GCT GGT GGA TCC ACA AAA CCC	235-255
10	D_atpB_as	GCG CGG GAT CCA CTG TGA CCA C**T**A CGG CAA C	868-838
11	D_atpB11_s	CGC AGG ATT A**G**A TAG GAC ACC	177-197
12	D_atpB11_as	GGT GTC CTA T**C**T AAT CCT GCG	197-177
13	ΔatpB-s	GTA ATT AAC AAC AAA GGG TAA TTT ACC AAC ACT ACT ACG	126-146/971-988
14	ΔatpB-as	CGT AGT AGT GTT GGT AAA TTA CCC TTT GTT GTT AAT TAC	988-971/146-126
15	atpB-AseI	GAA GAA CAT TAA TTT ACC AAC	959-979
16	atpF-C21A	GGC TGC CAT TAA TGG CGG CCA TAC GTA CTT CAT G**GC** GAA CAG AAC G	1413-1368
17	pET22-atpB-NdeI	*GAG ATA TAC ATA* TGG CTT CAG AAA ATA TGA CG	155-175
18	pET22-atpB-EcoRI	*GGA GCT CGA ATT C*TT AAT GTT CTT CAG ACG CC	970-952
19	pET-atpB-GTG-s-lang	CTG AAG CCA **C***AT GTA TAT CTC CTT C*	155-164
20	pET-atpB-GTG-as-lang	*GAA GGA GAT ATA CAT* **G**TG GCT TCA G	164-155
21	pET-atpB-TTG-s-lang	CTG AAG CCA **A***AT GTA TAT CTC CTT C*	155-164
22	pET-atpB-TTG-as-lang	*GAA GGA GAT ATA CAT* **T**TG GCT TCA G	164-155

Changes compared to the sequence of the wild type *atp* operon are in bold letters and underlined, whereas nucleotides of pET-22b are in italics. Numbering of the annealing region within the *atp* genes corresponds to plasmid pBWU13 starting with 1 at the second HindIII restriction site in *atpI*.

TABLE S2 Construction of plasmids

Plasmid	Vector fragment		Insert	Effect
	Vector	Vector or Template/Primer No.[a]	Site(s) used for Cloning	
pKH4 derivatives: *atp* genes are under control of the weak, constitutive *atp* promoter P3				
pBH12	pKH4	pBWU13	ScaI/EagI	WT *atp* operon
pBH13	pBH12	pBWU13 / 7+8	SspI	KpnI after P3 in *atpI*
pBRO1	pBH13	pJGA1 / 7+8	HindIII/SphI	Δ*atpB*
pJS1	pBH13	pBH13 / 9+10	BamHI	*a*W231end
pKK1	pBH13	pBH13 / 11+12	SspI	*a*Y11end
pBWU13 derivatives: *atp* genes are under control of the weak, constitutive *atp* promoter P3				
pBH2	pSTK3	pKH4	BssHII/EagI	Cys-less, His_6-β
				atpG: - BsrGI (silent)
pBH10	pBWU13	pBH2	RsrII/PmeI	*atpG*: - BsrGI (silent)
pJGA1	pBH10	pBWU13 / 13+14	HindIII/BsrGI	Δ*atpB*
pSTK3	pBWU13	pBWU13 / 15+16	AseI	*b*C21A
pBAD33 derivatives: *atp* genes are under control of the arabinose-inducible *araBAD* promoter				
pBAD33.atp	pBAD33	pBH13	KpnI/XbaI	WT *atp* operon
pBAD33.Δa	pBAD33.atp	pJS1	KpnI/XbaI	*a*W231end
pBAD33.Δa2	pBAD33.atp	pKK1	KpnI/XbaI	*a*Y11end
pBAB33.Δa3	pBAD33.atp	pBRO1	KpnI/XbaI	Δ*atpB*
pET-22b derivatives: *atpB* gene is under control of the IPTG-inducible T7-*laco* promoter				
pET22-atpB	pET-22b	pBWU13 / 17+18	NdeI/EcoRI	*a*, start codon ATG
pET22-atpB-GTG	pET22-atpB	pET22-atpB / 19+20	NcoI/SpHI	*a*, start codon GTG
pET22-atpB-TTG	pET22-atpB	pET22-atpB / 21+22	NcoI/SpHI	*a*, start codon TTG

Plasmids were obtained by cloning of corresponding inserts carrying the adequate mutations or by two-step PCR cloning. The numbers of the mutagenic primers used are given in the table, while the cloning primers correspond in each case to the restriction sites used for cloning.

[a] Primer sequences were listed with the corresponding number in Table S1.

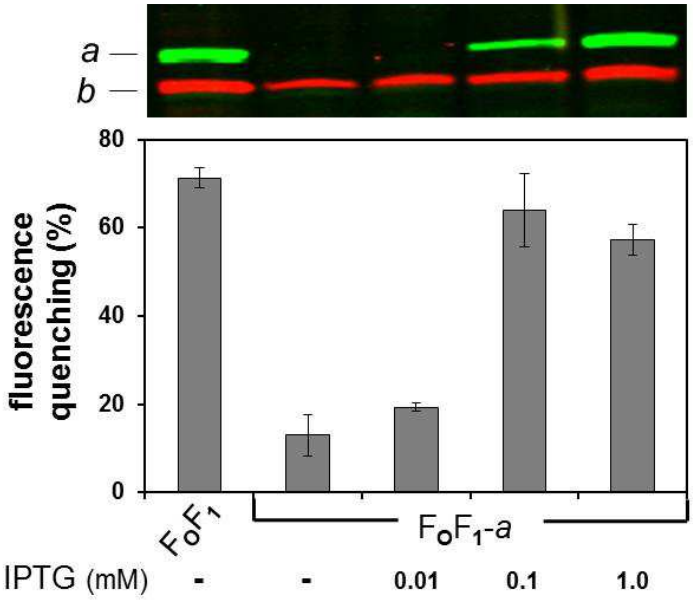

Figure S1. Induction of the T7-*laco* promoter controlling the expression of *atpB* by IPTG. DK8 transformed with pBAD33.atp, pET-22b, pT7POL26 (F_OF_1), and pBAD33.Δa3, pET22-atpB, pT7POL26 (F_OF_1-*a*; ATG), respectively, was grown as described in Fig. 3B using IPTG concentrations as indicated. Cells were harvested at OD = 0.8-1.0 and inverted membrane vesicles were prepared. Upper panel, immunoblot analysis of membrane vesicles (20 µg protein/lane). Immunolabeling was performed using monoclonal mouse anti-*a* (green) and polyclonal rabbit anti-*b* antibodies (red). Lower panel, ATP-driven proton translocation of membrane vesicles measured *via* ACMA fluorescence quenching. The relative magnitude of quenching induced by the addition of ATP is shown.

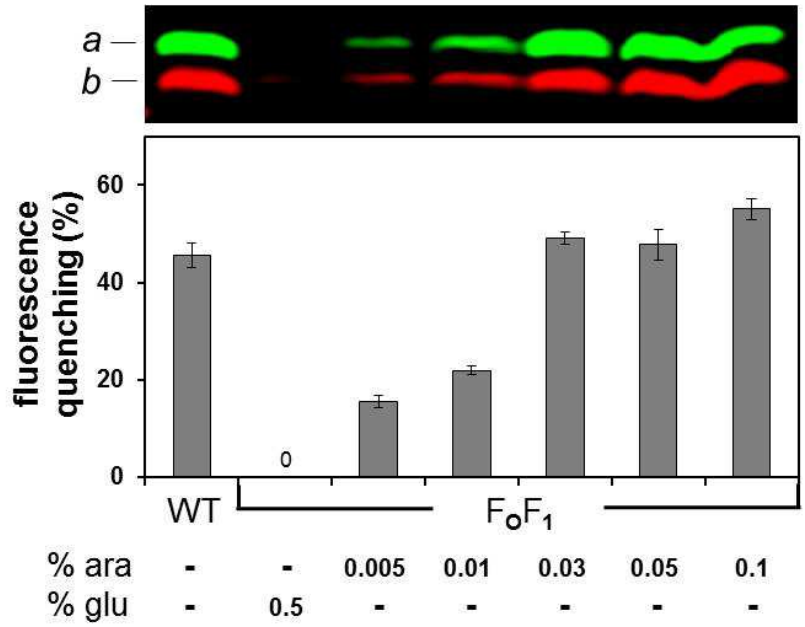

Figure S2. Induction of *araBADp* controlling expression of *atp* genes. Cells of *E. coli* DK8 transformed with pBWU13 (WT, control) and with pBAD33.atp, pET-22b, pT7POL26 (F_OF_1), respectively, were grown in LB medium supplemented with the corresponding antibiotics and with arabinose or glucose concentrations as indicated. Cells were harvested at OD = 0.8-1.0 and inverted membrane vesicles prepared. Upper panel, immunoblot analysis of membranes (20 µg protein/lane). Immunolabeling was performed using monoclonal mouse anti-*a* (green) or polyclonal rabbit anti-*b* antibodies (red). Lower panel, ATP-driven proton translocation of membrane vesicles measured *via* ACMA fluorescence quenching. The relative magnitude of quenching induced by the addition of ATP is shown. ara, arabinose; glu, glucose.

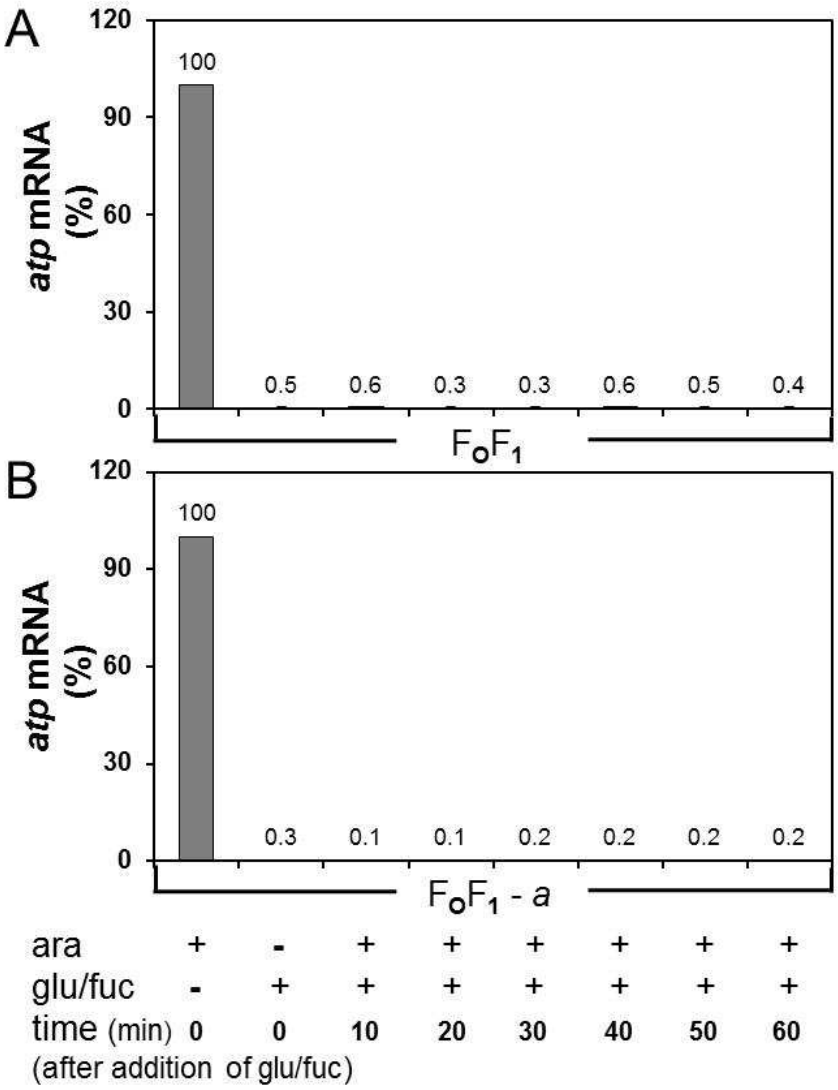

Figure S3. Degradation of *atp* mRNA after repression of *araBADp* controlling expression of *atpEFHAGDC* by glucose/D-fucose. DK8 carrying plasmids (A) pBAD33.atp, pET-22b, pT7POL26 (F_OF_1) or (B) pBAD33.Δa3, pET22-atpB-GTG, pT7POL26 (F_OF_1-*a*) was grown as described in Fig. 5. At each time point indicated, cells were harvested for isolation of total RNA. Real-time RT-PCR was performed using primer pair *atpE'F* (1/2). The amount of *atp* mRNA present in the samples grown in the presence of arabinose was set to 100 %. 100 % of F_OF_1-*a* corresponds to 54 % of F_OF_1 for *atpE'F* (1/2).